Magnetic field effects on the far-infrared absorption in Mn_{12}-acetate

A. B. Sushkov,* B. R. Jones, and J. L. Musfeldt*
Department of Chemistry, State University of New York at Binghamton, Binghamton, New York 13902-6016

Y. J. Wang
National High Magnetic Field Laboratory, Florida State University, Tallahassee, Florida 32306

R. M. Achey and N. S. Dalal
Department of Chemistry, Florida State University, Tallahassee, Florida 32310

(Received 15 December 2000; published 3 May 2001)

We report the far-infrared spectra of the molecular nanomagnet Mn_{12}-acetate (Mn_{12}) as a function of temperature (5–300 K) and magnetic field (0–17 T). The large number of observed vibrational modes is related to the low symmetry of the molecule, and they are grouped together in clusters. Analysis of the mode character based on molecular-dynamics simulations and model compound studies shows that all vibrations are complex; motion from a majority of atoms in the molecule contribute to most modes. Three features involving intramolecular vibrations of the Mn_{12} molecule centered at 284, 306, and 409 cm^{-1} show changes with applied magnetic field. The structure near 284 cm^{-1} displays the largest deviation with field and is mainly intensity related. A comparison between the temperature-dependent absorption-difference spectra, the gradual low-temperature cluster framework distortion as assessed by neutron-diffraction data, and field-dependent absorption-difference spectra suggests that this mode may involve Mn motion in the crown.

DOI: 10.1103/PhysRevB.63.214408 PACS number(s): 75.50.Xx, 68.49.Uv, 78.20.Ls

I. INTRODUCTION

Molecular magnet materials have attracted a great deal of interest in recent years, exhibiting fascinating properties such as cooperative phenomena, magnetic memory, quantum tunneling, and unusual relaxation behavior that are most commonly associated with mesoscopic solids. One prototypical single molecule magnet is $[Mn_{12}O_{12}(CH_3COO)_{16}(H_2O)_4]\cdot 2CH_3COOH\cdot 4H_2O$, denoted as Mn_{12}. It consists of eight Mn^{3+} ($S=2$) and four Mn^{4+} ($S=3/2$) ions, held together by oxygen atoms, acetate ligands, and waters of crystallization; the ferrimagnetic spin arrangement yields $S=10$.[1] Mn_{12} crystallizes in a tetragonal lattice, with weak exchange coupling and no long range magnetic ordering.[2–4] Though a number of efforts have been made to understand the energetics of the Mn_{12} system, a quantitative theory is still lacking. Recent prospective Hamiltonians include anisotropy, Zeeman splitting, spin-phonon interaction, and transverse terms, as well as spin operators up to fourth order.[5–8]

Mn_{12} initially attracted attention due to the striking steps and hysteresis loop in the magnetization, indicative of quantum tunneling.[9] At present, these steps are thought to result from the double-well potential that separates spin states; magnetization reorientation transitions have optimal probability when the ''spin-up'' and ''spin-down'' levels of the different magnetic quantum numbers align with applied magnetic field.[9–15] High field electron-paramagnetic-resonance,[16,17] neutron scattering,[18] and sub-mm[19] techniques have been used to measure the excitation energies between levels in these magnetic clusters. The highest energy excitation ($m_s=10\rightarrow m_s=9$) occurs in the very far infrared, near 10 cm^{-1} (300 GHz). That the magnetic dipole transition energies in the Mn_{12} system are irregular (especially near the top of the anisotropy barrier) clearly shows the presence of higher than second-order terms in the spin Hamiltonian.[16,18] Early heat-capacity measurements revealed the irreversible/reversible effects between the two wells below/above the blocking temperature.[20] The exact value of the blocking temperature T_b (≈ 3 K) depends on the probe, due to the dynamic nature of the blocking process. Above 3 K, the magnetization relaxation is exponential in time and reversible; this is the thermally activated regime. Notable deviations from exponential relaxation are observed below 2 K.[21]

Despite an explosion of interest in the low-energy quantum behavior, little is known about the vibrational characteristics of Mn_{12} and many other prototypical molecular magnet materials. Spin-phonon coupled modes have been investigated in other transition-metal oxides such as EuO, $LaMnO_3$, α'-NaV_2O_5, and CuO; the frequencies at which they appear correspond to vibrational modulation of the superexchange integral in the materials,[22–27] rather than the aforementioned low-energy, phonon-assisted relaxation processes. In order to provide further information on the electrodynamic response of single-molecule molecular magnets, we have measured the far-infrared spectra of Mn_{12} as a function of both temperature and applied magnetic field in the thermally activated regime. We use this data to assess spin-phonon coupling in this material.

II. EXPERIMENT

High-quality single crystals of Mn_{12} were synthesized following the original procedure described by Lis.[2] The single crystals of Mn_{12} were ground with paraffin at 77 K to prepare pellets of various concentrations suitable for transmittance measurements in the far infrared.[28] A sample with

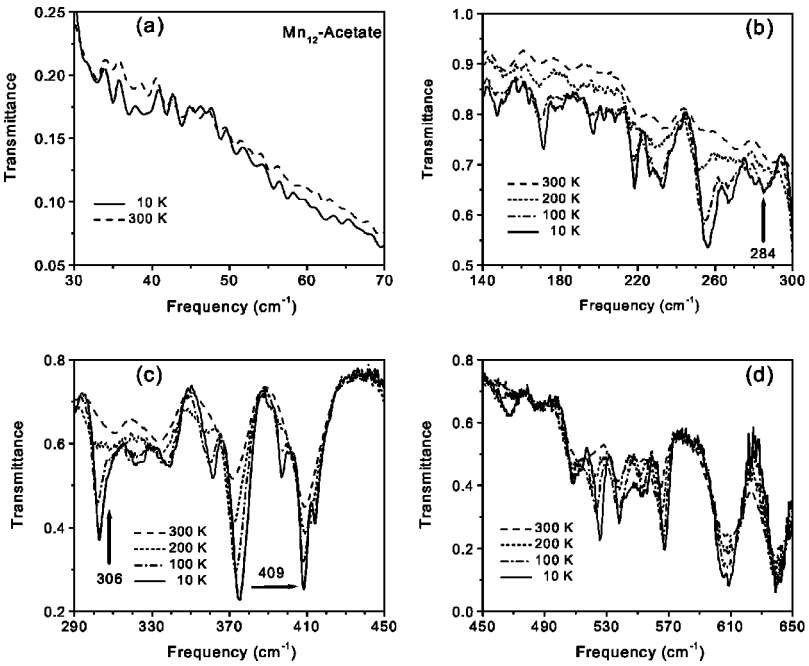

FIG. 1. Far-infrared transmittance spectra of 85% by mass (a) and 3.5% by mass [(b), (c), and (d)] Mn_{12} suspended in a paraffin pellet at various temperatures (10, 100, 200, and 300 K). Arrows indicate the three magnetic-field-dependent features at 284, 306, and 409 cm^{-1}.

$\approx 3.5\%$ Mn_{12} by mass proved to be optimal for most of the frequency range under investigation. A more concentrated pellet ($\approx 85\%$) was used for measurements between 30 and 110 cm^{-1}.

Infrared transmission measurements were performed in our laboratory and at the National High Magnetic Field Laboratory (NHMFL) in Tallahassee, Florida, using a Bruker 113V Fourier-transform infrared spectrometer. Spectra were taken using the 3.5-, 12-, 23-, and 50-μm mylar beam splitters, covering a frequency range of 25–650 cm^{-1}. Both absolute and relative transmittance spectra were measured as a function of temperature using a bolometer detector and a continuous flow helium cryostat. Small differences in the transmittance spectra were assessed at low temperature using absorption differences, calculated from the relative transmittance as $\alpha(T)-\alpha(T=5\ \mathrm{K})=-\ln[\mathcal{T}(T)/\mathcal{T}(T=5\ \mathrm{K})]$. The magnetic-field dependence of the transmittance at 5 K was measured at the NHMFL using a 20-T superconducting magnet and a transmission probe equipped with a bolometer detector.[29,30] Again, transmittance ratio spectra were used to investigate small deviations from unity due to the applied field. By taking the natural log of the transmittance ratio $(-\ln[\mathcal{T}(H)/\mathcal{T}(H=0)])$, we obtain the absorption difference at each field: $\alpha(H)-\alpha(H=0)$.

Upon examination of the absorption-difference curves over the entire aforementioned frequency range, we identified three features that change with applied magnetic field. In order to distinguish signal from noise in a quantitative way, we calculated the standard deviation from the mean for each feature. In addition, the same analysis was performed on representative nearby frequency ranges containing no obvious field-dependent features. We use these standard deviations from the mean to quantify the effects of the field and to characterize the intrinsic noise level in regimes away from the magneto-optic signatures.[31] Field sweeps on an empty hole were also carried out for reference; as expected, no field dependence was observed.

III. RESULTS AND DISCUSSION

A. Temperature dependence of the far-infrared vibrational spectra

Figure 1 displays the far-infrared transmittance of Mn_{12} as a function of temperature. As expected for a molecular solid, intramolecular vibrational modes of the Mn_{12} molecule appear above 150 cm^{-1}.[32] In agreement with previous authors,[19,33] we also observe a weak low-energy structure centered near 35 cm^{-1} [Fig. 1(a)]. This magnetic dipole-allowed excitation has been cited as evidence for other excited-state multiplets with $S \neq 10$ existing in Mn_{12}.[19,33] Within our sensitivity, we have found that the 35-cm^{-1} feature displays limited temperature dependence and no magnetic-field dependence.

The far-infrared spectra of Mn_{12} display a large number of intramolecular modes due to the relatively low symmetry of the molecule. They are grouped together in clusters and superimposed upon one another. These structures sharpen and harden with decreasing temperature (Fig. 1). Recent 20-K neutron-diffraction studies by Langan *et al.*[3] assessed the low-temperature molecular distortion; compared to the 300-K structure, major characteristics include a gradual displacement of Mn(3) and carboxylate groups, and more extensive solvent interactions including a four-center hydrogen bond. [Note that Mn(3) is part of the crown, according to the numbering scheme of Ref. 3, with connections/interactions to the bridges, ligands, and solvent.] These results motivated us to more carefully investigate the far-infrared response in the low-temperature regime.

Figure 2(a) displays the absorption-difference spectra of Mn_{12} at low temperature.[34] The gradual distortion of the

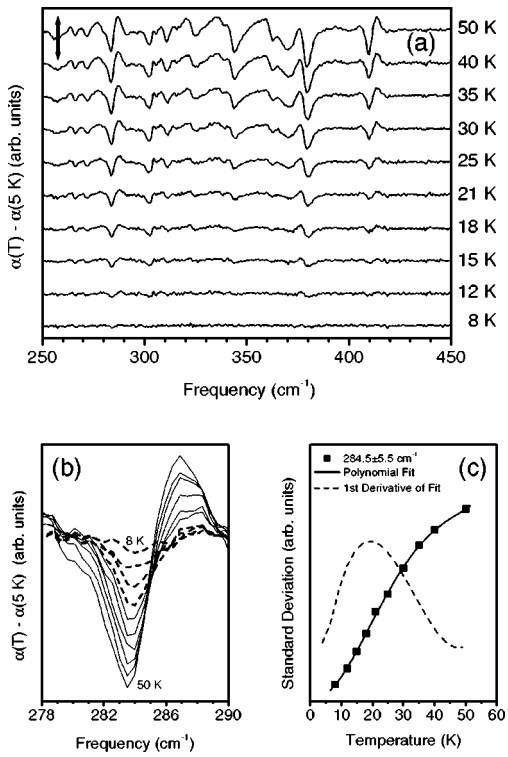

FIG. 2. (a) Far-infrared absorbance-difference spectra $[\alpha(T) - \alpha(T=5\ \mathrm{K})]$ of Mn_{12} as a function of frequency at low temperature. The curves are offset for clarity. The arrow indicates 10% deviation from unity. (b) Close-up view of the absorbance-difference spectra near the 284-cm^{-1} feature at low temperature. Dashed lines: temperatures below 20 K; solid lines: temperatures above 20 K. (c) Standard deviation from the mean of the 284-cm^{-1} absorbance difference. Solid line: fourth-order polynomial fit to guide the eye; dashed line: derivative of fourth-order polynomial fit.

cluster framework was previously assessed by neutron-diffraction studies.[3] The behavior of the Mn ions at low temperature is most important to the magnetic properties of Mn_{12}; the neutron diffraction experiments indicate that Mn(3) on the crown displays the most significant displacement.[3] A number of vibrational features are modified in this temperature range and are therefore likely to contain a substantial Mn(3), carboxylate, and acetate ligand contribution. As will be discussed in the next section, three modes (284, 306, and 409 cm^{-1}) are of particular interest because of their dependence on magnetic field. The 284-cm^{-1} mode shows an intensity variation at low temperature and a small frequency shift at higher temperatures [Fig. 2(b)]. The standard deviation from the mean in the vicinity of the 284-cm^{-1} feature [Fig. 2(c)] quantifies these changes, with an inflection point around 20 K. The maximum in the derivative of the fourth-order polynomial fit to this data better illustrates the position of this inflection point. The 306-cm^{-1} structure (not shown) is sensitive to this temperature regime as well. Although the feature centered at 409 cm^{-1} also exhibits changes in this temperature range, no peculiarities were observed around 20 K.

Preliminary molecular-dynamics simulations[35] suggest that a majority of atoms in the Mn_{12} molecule are, in some

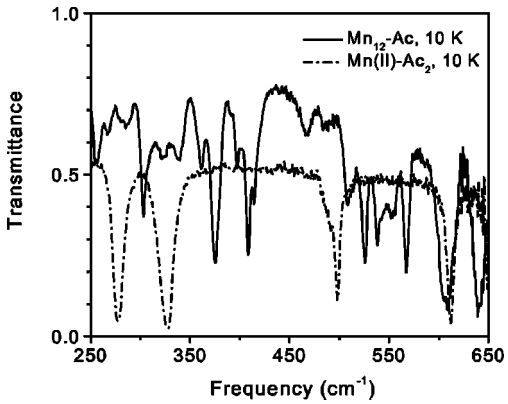

FIG. 3. Far-infrared transmittance spectra of Mn_{12} alongside similar data on the model compound Mn(II)-Ac_2. Spectra were collected at 10 K.

way, involved in each vibration in this frequency range. The modes are many, both because of the low molecular symmetry and the large number of atoms. Using mode visualization and the spectra of several model compounds as a guide, particularly that of Mn(II)-Ac_2 (Fig. 3), we propose the following general assignments. The low-energy motions below 300 cm^{-1} include a great deal of acetate (ligand) motion. Complex low-energy motions of the core and crown begin around 180 cm^{-1}. These motions include bending, rocking, shearing, twisting, and wagging. Asymmetric and symmetric stretching of the core and crown seem to begin slightly below 500 cm^{-1}, thus providing a likely assignment for the complicated vibrational cluster observed in the spectrum centered near 540 cm^{-1}. The simulations show that modes in this energy range contain sizable (core and crown) oxygen contributions. Comparison of the spectral data from the model compound Mn(II)-Ac_2 and from Mn_{12} confirm that the mode clusters centered near 360, 400, and 540 cm^{-1} in Mn_{12} are mainly motions of the magnetic center rather than the ligands. Related model compounds such as MnO, MnO_2, and Mn_2O_3 also have characteristic vibrational features in the far infrared (below 600 cm^{-1}). Although the structures are different and have unmixed Mn valences compared to the title compound, the reference spectra of these model Mn-based solids[36] indicate that the far-infrared response is rich and highly relevant to the Mn-O motion. Measurements on the Mn(II)-Ac_2 model compound (Fig. 3) suggest that the structures centered at 590 and 635 cm^{-1} in the spectrum of Mn_{12} are acetate related. The similar temperature dependence of these modes in the two samples supports this assignment.

In order to understand and model physical properties that contain important phonon contributions (for instance ρ_{DC} or heat capacity) in the thermally activated regime, it is helpful to know realistic values of the most important low-energy infrared-active phonons of Mn_{12}. Our data suggests that use of a relatively small series of characteristic frequencies may be adequate. For instance, the three most intense structures are centered at 375, 410, and 540 cm^{-1}. More complete models might take additional modes, the detailed mode clustering, and relative intensities into account.

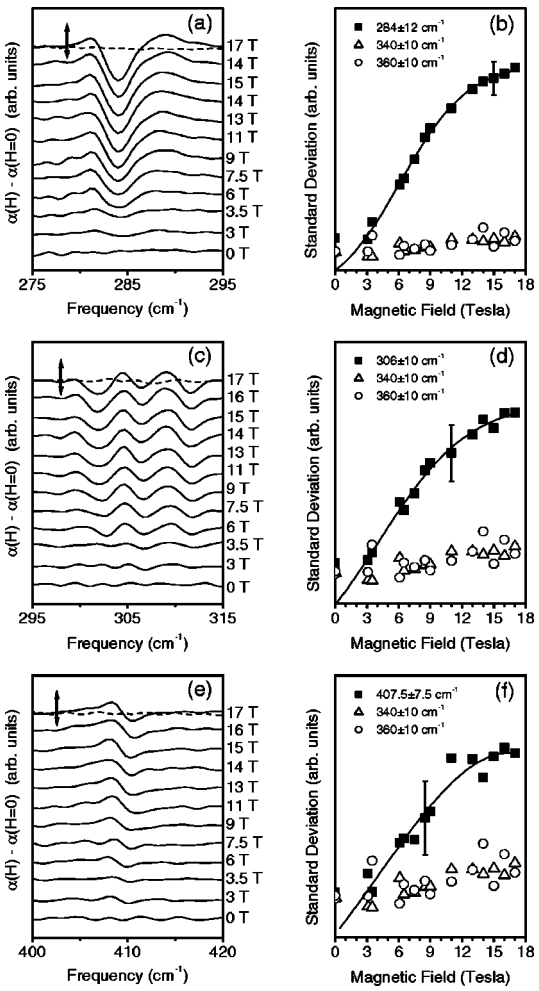

FIG. 4. Magnetic-field-dependent features in absorbance-difference spectra at 5 K. Left column of plots: $\alpha(H)-\alpha(H=0)$ vs frequency at different magnetic fields (curves are shifted for clarity) for features at 284 (a), 306 (c), and 409 cm^{-1} (e). Solid curves: sample; dashed curve: empty reference (hole). Arrows indicate 5% deviation from unity. Right column: standard deviation from the mean value vs magnetic field calculated for the frequency intervals indicated on the plots [(b), (d), and (f)]. Solid lines guide the eye.

B. Magnetic-field dependence of the far-infrared vibrational spectra

Figure 4 displays the magnetic-field dependence of three features in the far-infrared spectrum of Mn_{12}. The center positions of these structures ($\approx$284, 306, and 409 cm^{-1}) are indicated with arrows on the absolute-transmittance spectra in Fig. 1. It is interesting that the 284- and 306-cm^{-1} features do not correspond to major modes in the absolute-transmittance spectrum. As shown in the left-hand panels [Figs. 4(a), 4(c), and 4(e)], the field dependence as measured by the absorption-difference spectra is well defined for the mode near 284 cm^{-1}, whereas it is more modest for the structures centered at 306 and 409 cm^{-1}. The filled symbols and solid lines in the right-hand panels [Figs. 4(b), 4(d), and 4(f)] provide a quantitative view of the field-dependent trends. The standard deviation from the mean for the three modes of interest shows a clear upward trend, in contrast to that of nearby spectral regions that show no field dependence and provide an estimate of the intrinsic noise level.[37]

The feature at 284 cm^{-1} is the most prominent of the three field-dependent structures. The absorption decreases with applied field and shows a tendency toward saturation at 17 T, as indicated in Fig. 4(b). The standard deviation from the mean in nearby spectral ranges (for instance, similarly sized regimes centered at $\approx$340 and 360-cm^{-1}) shows no field dependence. The response of the 284-cm^{-1} feature is therefore well above the noise and characteristic of Mn_{12}. Similar trends and a tendency towards saturation of the standard deviation from the mean are observed for the more complicated absorption-difference structures centered near 306 and 409 cm^{-1}, although the overall coupling of these modes to the applied field is weaker and the line shapes are different from that of the 284-cm^{-1} feature. The changes observed near 306 cm^{-1} are mainly caused by a 1-cm^{-1} softening, whereas the 409-cm^{-1} structure is due to both softening and broadening. The field dependence of these three features in the absorption-difference spectra is confirmed by repeated measurements using different experimental parameters.[38] Further, as seen in Fig. 4, the trend with applied field in both the difference spectra and the standard deviation from the mean near 306 and 409 cm^{-1} can be easily distinguished from that of the non-field-dependent intervals.

It is of interest to understand the microscopic character of the 284-, 306-, and 409-cm^{-1} modes and why they are affected by the magnetic field. Although there are a number of mechanisms that might explain this behavior, such as the effect of magnetic field on hybridization of ligand-metal bonds,[39] Dzyaloshinsky-Moriya interactions,[40,41] and the effect of field on Jahn-Teller modes,[42,43] we believe the most promising is that of spin-phonon coupling. Here, variations in the applied field modulate the magnetic system, thereby affecting the phonons coupled to it. Such an interaction has been thought to be important for describing the slow magnetization relaxation behavior of Mn_{12}, making it an important term in the total Hamiltonian.[7,8] That only three far-infrared features are observed to change with applied field up to 17 T suggests that these modes are related to motions that maximally change the low-temperature spin interactions. One possible candidate for such motion might contain bending between the core and crown structures affecting the Mn-O-Mn angle, therefore modulating the superexchange between Mn ions. An alternate explanation involves the especially curious sensitivity of the 284-cm^{-1} mode to temperature variation (in the range 5–35 K) as well as to the applied magnetic field. This coincidence suggests that the magnetoelastic response at 284 cm^{-1} may be intimately related to the Mn(3) motion on the crown. Interestingly, the 306-cm^{-1} structure also displays some sensitivity to the displacement of the molecular framework. Further work is clearly needed to untangle these complex interactions.

The observed magnetic-field dependencies at 284, 306, and 409 cm^{-1} suggest that $\mathcal{H}_{s-ph}$ can be augmented by including contributions from these three vibrational modes. Spin-lattice interactions in the far-infrared energy range have been observed in a number of other transition-metal oxides

in the past.[22–27] However, the energy scale of the 284-, 306-, and 409-cm^{-1} features is larger than might be expected for relevant spin-phonon processes in Mn_{12}, even in the thermally activated regime. Indeed, previous studies on the title compound have focused on acoustic phonons as the major contributors to $\mathcal{H}_{s-ph}$.[5] Thus, if these far-infrared phonons are connected with the Mn_{12} relaxation processes in any way, virtual states would likely be involved. The energy scale of the 284-, 306-, and 409-cm^{-1} phonons may be more relevant to high-field transport or specific-heat measurements.

IV. CONCLUSION

We have measured the far-infrared response of Mn_{12} as a function of temperature and magnetic field. The features in this region involve vibrations from all of the groups of atoms (core, crown, and ligands) in the molecule. Three structures related to intramolecular vibrations near 284, 306, and 409 cm^{-1} are observed to change in applied magnetic field, suggesting that they are coupled to the spin system. Of these three, the feature centered at 284 cm^{-1} displays the strongest coupling. Based on the similarity between the temperature- and field-dependent absorption-difference data, we speculate that this mode involves Mn(3) motion on the crown. The data reported here may be helpful in understanding the role of vibrations in the theoretical models of magnetization relaxation in Mn_{12} and related systems.

ACKNOWLEDGMENTS

Funding from the National Science Foundation (Grant No. DMR-9623221) to support work at SUNY Binghamton is gratefully acknowledged. The work at Florida State University was also partially supported by the NSF. A portion of the measurements were performed at the NHMFL, which is supported by the NSF Cooperative Agreement Grant No. DMR-9527035 and by the State of Florida. We thank Z.T. Zhu for technical assistance.

*Present address: Department of Chemistry, University of Tennessee, Knoxville, TN 37996.

[1] G. Christou, D. Gatteschi, D.N. Hendrickson, and R. Sessoli, MRS Bull. **25**, 66 (2000).
[2] T. Lis, Acta Crystallogr., Sect. B: Struct. Crystallogr. Cryst. Chem. **B36**, 2042 (1980).
[3] P. Langan, R.A. Robinson, P.J. Brown, D.N. Argyriou, D.N. Hendrickson, and S.M.J. Aubin (unpublished).
[4] R.A. Robinson, P.J. Brown, D.N. Argyriou, D.N. Hendrickson, and S.M.J. Aubin, J. Phys.: Condens. Matter **12**, 2805 (2000).
[5] T. Pohjola and H. Schoeller, Phys. Rev. B **62**, 15 026 (2000).
[6] M.N. Leuenberger and D. Loss, Phys. Rev. B **61**, 1286 (2000).
[7] P. Politi, A. Rettori, F. Hartmann-Boutron, and J. Villain, Phys. Rev. Lett. **75**, 537 (1995).
[8] A. Fort, A. Rettori, J. Villain, D. Gatteschi, and R. Sessoli, Phys. Rev. Lett. **80**, 612 (1998).
[9] J.R. Friedman, M.P. Sarachick, J. Tejada, and R. Ziolo, Phys. Rev. Lett. **76**, 3830 (1996).
[10] B. Barbara, W. Wernsdorfer, L.C. Sampaio, J.G. Park, C. Paulsen, M.A. Novak, R. Ferré, D. Mailly, R. Sessoli, A. Caneschi, K. Hasselbach, A. Benoit, and L. Thomas, J. Magn. Magn. Mater. **140-144**, 1825 (1994).
[11] R. Sessoli, D. Gatteschi, A. Caneschi, and M.A. Novak, Nature (London) **365**, 141 (1993).
[12] L. Thomas, F. Lionti, R. Ballou, D. Gatteschi, R. Sessoli, and B. Barbara, Nature (London) **383**, 145 (1996).
[13] J.R. Friedman, M.P. Sarachik, J. Tejada, J. Maciejewski, and R. Ziolo, J. Appl. Phys. **79**, 6031 (1996).
[14] J.R. Friedman, M.P. Sarachik, J.M. Hernandez, X.X. Zhang, J. Tejada, E. Molins, and R. Ziolo, J. Appl. Phys. **81**, 3978 (1997).
[15] E. del Barco, J.M. Hernandez, M. Sales, J. Tejada, H. Rakoto, J.M. Broto, and E.M. Chudnovsky, Phys. Rev. B **60**, 11 898 (1999).
[16] S. Hill, J.A.A.J. Perenboom, N.S. Dalal, T. Hathaway, T. Stalcup, and J.S. Brooks, Phys. Rev. Lett. **80**, 2453 (1998).
[17] A.L. Barra, D. Gatteschi, and R. Sessoli, Phys. Rev. B **56**, 8192 (1997).
[18] I. Mirebeau, M. Hennion, H. Casalta, H. Andres, H.U. Güdel, A.V. Irodova, and A. Caneschi, Phys. Rev. Lett. **83**, 628 (1999).
[19] A.A. Mukhin, V.D. Travkin, A.K. Zvezdin, S.P. Lebedev, A. Caneschi, and D. Gatteschi, Europhys. Lett. **44**, 778 (1998).
[20] F. Fominaya, J. Villian, P. Gandit, J. Chaussy, and A. Caneschi, Phys. Rev. Lett. **79**, 1126 (1997).
[21] M. Evangelisti, J. Bartolomé, and F. Luis, Solid State Commun. **112**, 687 (1999).
[22] W. Baltensperger and J.S. Helman, Helv. Phys. Acta **41**, 668 (1968).
[23] E. Granado, A. García, J.A. Sanjurjo, C. Rettori, I. Torriani, F. Prado, R.D. Sánchez, A. Caneiro, and S.B. Oseroff, Phys. Rev. B **60**, 11 879 (1999).
[24] V.B. Podobedov, A. Weber, D.B. Romero, J.P. Rice, and H.D. Drew, Phys. Rev. B **58**, 43 (1998).
[25] E.Y. Sherman, M. Fischer, P. Lemmens, P.H.M. van Loosdrecht, and G. Güntherodt, Europhys. Lett. **48**, 648 (1999).
[26] A.B. Kuz'menko, D. van der Marel, P.J.M. van Bentrum, E.A. Tischenko, C. Presura, and A.A. Bush, Physica B **284-288**, 1396 (2000).
[27] A.B. Kuz'menko, D. van der Marel, P.J.M. van Bentum, E.A. Tishchenko, C. Presura, and A.A. Bush, Phys. Rev. B **63**, 094303 (2001).
[28] Note that this process results in an isotropic sample.
[29] H.K. Ng and Y.J. Wang, *Physical Phenomena at High Magnetic Fields II*, edited by Z. Fisk, L. Gor'kov, D. Meltzer, and R. Schrieffer (World Scientific, Singapore, 1995), p. 729.
[30] The field dependence was measured in the following order: 0, 9, 13, 15, 17, 16, 14, 11, 8.5, 6.5, 3.5, 0, 3, 6, 7.5, and 0 T. No hysteresis was observed.
[31] Standard deviation from the mean was used to quantify the features in the absorbance-difference spectra rather than integrated intensity due to the complicated line shapes of some of the features. This method was also used to estimate the intrinsic noise level by analysis of nearby spectral regions. Thus, for consistency, standard deviation from the mean was used for all treatments of the difference spectra.

[32] M.S. Dresselhaus, G. Dresselhaus, and P.C. Eklund, *Science of Fullerenes and Carbon Nanotubes* (Academic Press, New York, 1996).
[33] M. Hennion, L. Pardi, I. Mirebeau, E. Suard, R. Sessoli, and A. Caneschi, Phys. Rev. B **56**, 8819 (1997).
[34] This temperature range is relevant to the energy scale of the magnetic measurements.
[35] Molecular-dynamics simulations were performed using the MMFF method of the TITAN computer program by Schrodinger, Inc.
[36] *The Stadtler Standard Spectra, Inorganics and Related Compounds, IR Grating Spectra* (Stadtler Research Laboratories, Philadelphia, 1972).
[37] The method for determining the standard deviation from the mean is described in Sec. II.
[38] The field dependences of these three features were confirmed by repeating the measurements using different (yet valid) scan velocities and beam splitters.
[39] L.C. Brunel, G. Landwehr, A. Bussmann-Holder, H. Bilz, M. Balkanski, M. Massot, and M.K. Ziolkiewicz, J. Phys. (France) **42**, 412 (1981).
[40] M.I. Katsnelson, V.V. Dobrovitski, and B.N. Harmon, Phys. Rev. B **59**, 6919 (1999).
[41] O. Cépas, K. Kakurai, L.P. Regnault, T. Ziman, J.P. Boucher, N. Aso, M. Nishi, H. Kageyama, and Y. Ueda (unpublished).
[42] A. Garg, Phys. Rev. Lett. **81**, 1513 (1998).
[43] S.M.J. Aubin, Z. Sun, H.J. Eppley, E.M. Rumberger, I.A. Guzei, K. Folting, P.K. Gantzel, A.L. Rheingold, G. Christou, and D.N. Hendrickson (unpublished).